Supporting Information

# Chemical communication in spatially organized protocell colonies and protocell/living cell micro-arrays

Xuejing Wang[† a,b], Liangfei Tian[† b], Hang Du[a], Mei Li[b], Wei Mu[a], Bruce W. Drinkwater[c], Xiaojun Han*[a], and Stephen Mann*[b]

[a.] State Key Laboratory of Urban Water Resource and Environment School of Chemistry and Chemical Engineering, Harbin Institute of Technology, Harbin, China, 150001, E-mail: hanxiaojun@hit.edu.cn
[b.] Centre for Protolife Research and Centre for Organized Matter Chemistry, School of Chemistry University of Bristol, Bristol, BS8 1TS UK, E-mail: s.mann@bristol.ac.uk
[c.] Faculty of Engineering, University of Bristol, Bristol, BS8 1TR UK

**Description of Movies**

**Movie S1**. Fluorescence microscopy video showing the dynamic and reversible modulation of the GUVs array from horizontal to vertical or 1D to 2D arrays by periodically (ca. 30 s) switching on/off the corresponding pairs of piezoelectric transducers. The GUV array was prepared by adding 30 μL of sucrose containing GUVs (400 mM) to isotonic glucose solution (1 mL, 400 mM). Movie is shown at x30 of real-time speed at 5 frames per second. Total duration of recording was 3 minutes in real time.

**Movie S2.** Fluorescence microscopy video showing the dynamic and reversible modulation of the hybrid hemifused (red GUVs)/non-hemifused GUVs (green GUVs) array by switching on/off the corresponding pairs of piezoelectric transducers. A 2D array of TR-DHPE labelled GUVs (red) was first prepared by adding 30 μL of sucrose containing GUVs (400 mM) to isotonic glucose solution (1 mL, 400 mM) in the presence of a 2D acoustic pressure field (5.06/9.13 MHz, 10 V), and hemifused by the additional of $CaCl_2$ (10 μL, 133 mM) in the same acoustic pressure field. Then, the supernatant in the acoustic trapping chamber was carefully replaced by glucose solution (400 mM) to remove the $Ca^{2+}$. The hemifused/non-hemifused hybrid GUV array was obtained by the additional of 20 μL of sucrose containing NBD-PE labelled GUV (green) to the acoustic trapping chamber. To control dynamic modulation of the GUV arrays, the two orthogonal pairs of transducers were switched on/off about every 60 s. Movie is shown at x38 of real-time speed at 4 frames per second. Total duration of recording was 3 minutes in real time.

## Supplementary Figures

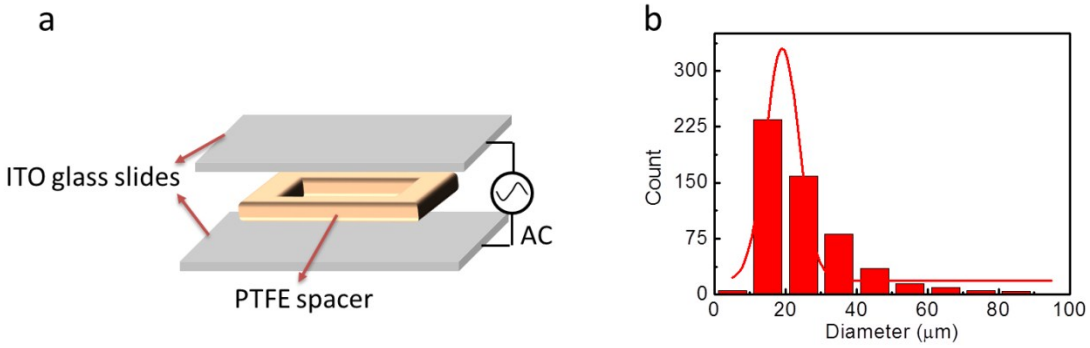


**Figure S1.** (**a**) Schematic representation of the experimental setup for GUVs electroformation. (**b**) Histogram of GUV diameters for samples prepared by electroformation.

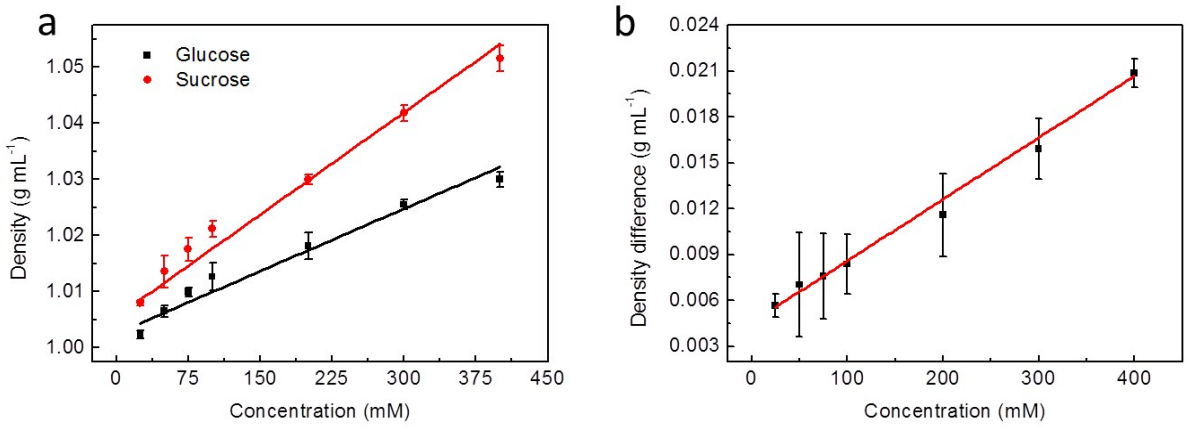


**Figure S2.** (**a**) Plots of the density of sucrose (red) and glucose (black) aqueous solutions against concentration (5-400 mM). (**b**) Plot of the density difference between sucrose and glucose against concentration. Three independent replicates were conducted in sucrose and glucose concentration. Error bars represent the standard deviation.

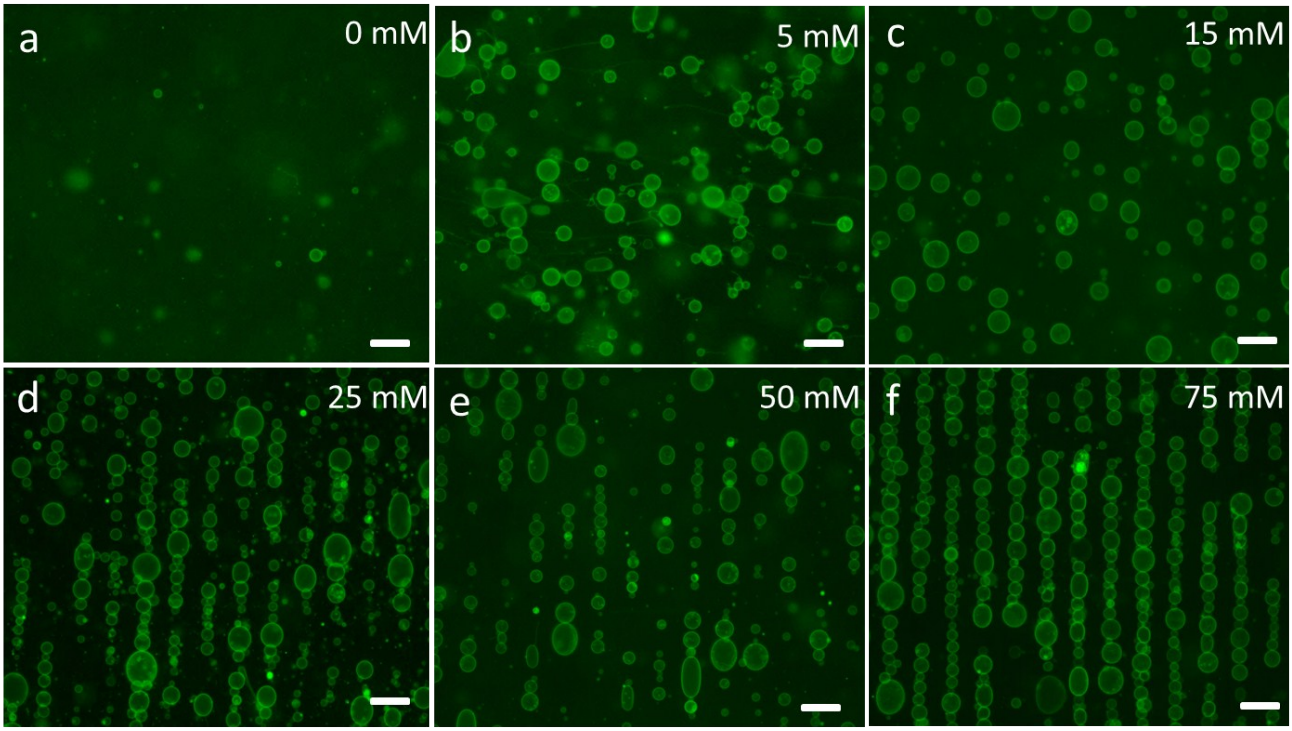


**Figure S3.** Representative fluorescence microscopy images of DPOC GUVs prepared with different internal sucrose/external glucose isotonic concentrations in a 1D acoustic pressure field (9.13 MHz, 10 V): (**a**) no sugars (0 mM), (**b**) 5, (**c**) 15, (**d**) 25, (**e**) 50 and (**f**) 75 mM. The GUVs were prepared by electroformation using DOPC and 5% NBD-PE (green fluorescence). All scale bars are 100 μm.

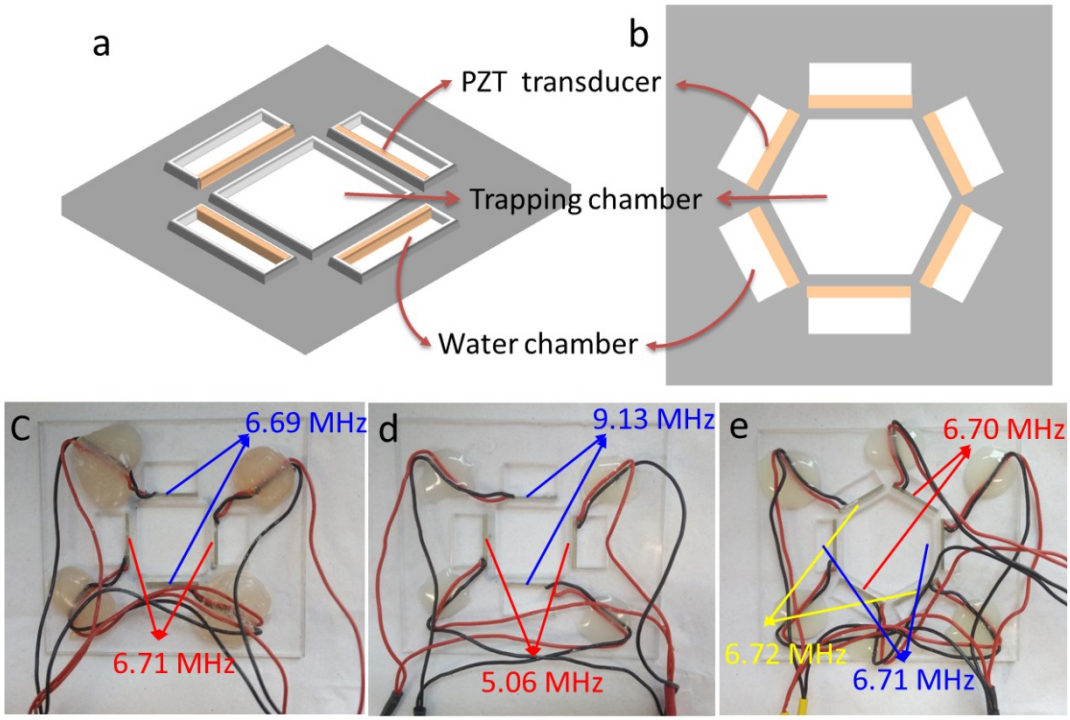


**Figure S4.** (**a-b**) Schematic representation of the customer-made square (**a**) and hexagon (**b**) shaped acoustic trapping devices. (**c-e**) Photos of the custom-built square (**c** and **d**) and hexagon (**e**) shaped acoustic trapping devices. The trapping devices were constructed from poly(ethyleneterephthalate) (PET) and four (**c** and **d**) or six (**e**) piezoelectric transducers oriented as two or three orthogonal pairs operating at similar or different resonance frequencies. Each transducer was attached with adhesive to the back of the central square chamber with cyanoacrylate, and the four or six rectangular chambers surrounding the central sample chamber were used to store water to provide cooling. A BSA-modified glass coverslip was attached with adhesive to the bottom of the device. Trapping of the sucrose-containing GUVs in isotonic glucose occurred on the bottom surface of the device. The device was re-used by replacing the BSA-modified glass coverslip.

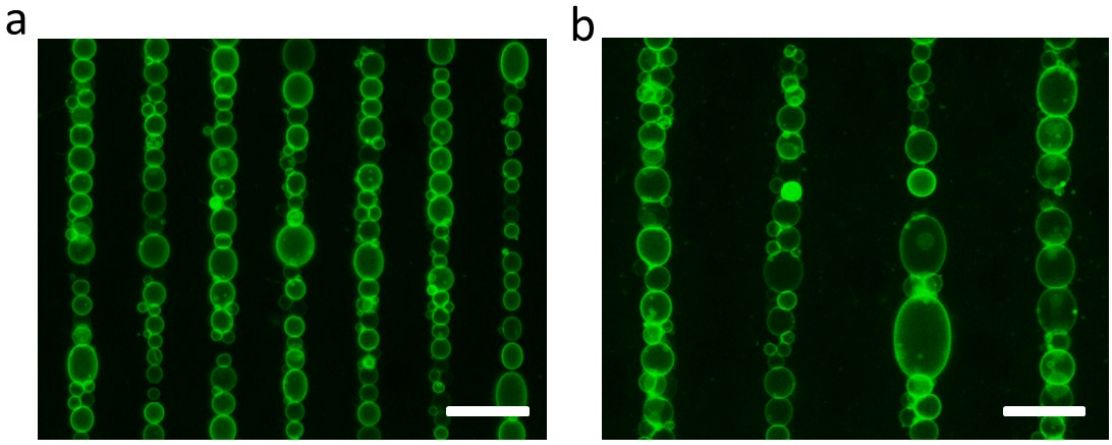


**Figure S5.** Representative fluorescence microscopy images of a 1D DOPC GUV micro-array in acoustic fields produced at different resonance frequencies; (**a**) 9.13MHz, and (**b**) 5.06 MHz. The GUVs contained sucrose and were prepared in isotonic glucose from DOPC with 5% NBD-PE. The line spacings were adjusted to 110 or 146 μm at 6.71 or 5.06 MHz, respectively. All scale bars are 100 μm.

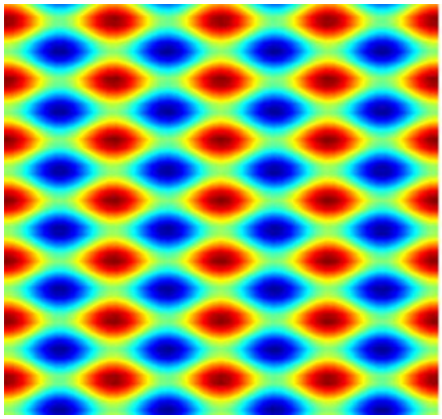

**Figure S6.** Simulation of the acoustic pressure distribution in the acoustic trapping device for two pairs of PZTs with a square arrangement operating at 5.06/9.13 MHz displaying a rectangular lattice; high pressure (blue), low pressure (red).

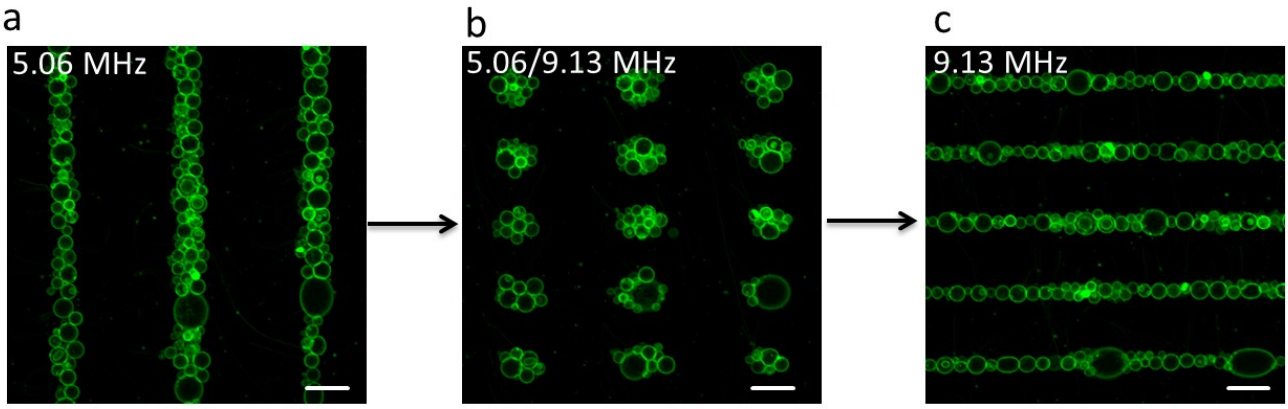


**Figure S7**. Representative fluorescence microscope images of dynamically modulated DOPC GUVs (5% NBD-PE) array from 1D array at 5.06 MHz (**a**) to 2D array at 5.06/9.13 MHz (**b**), and to 9.13 MHz (**c**). Scale bars are 50 μm.

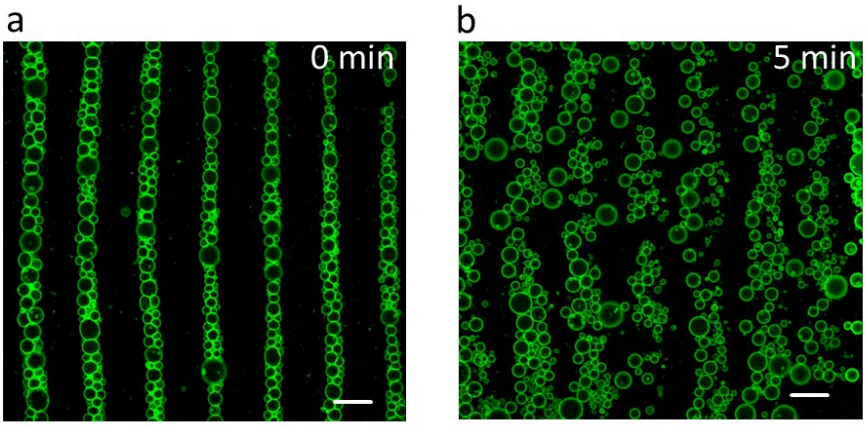


**Figure S8**. Representative fluorescence microscopy images of 1D DOPC (5% NBD-PE) GUVs micro-array in acoustic fields produced at 5.06 MHz before (**a**) and after (**b**) switching off the acoustic field for 5 min. Scale bars are 100 μm.

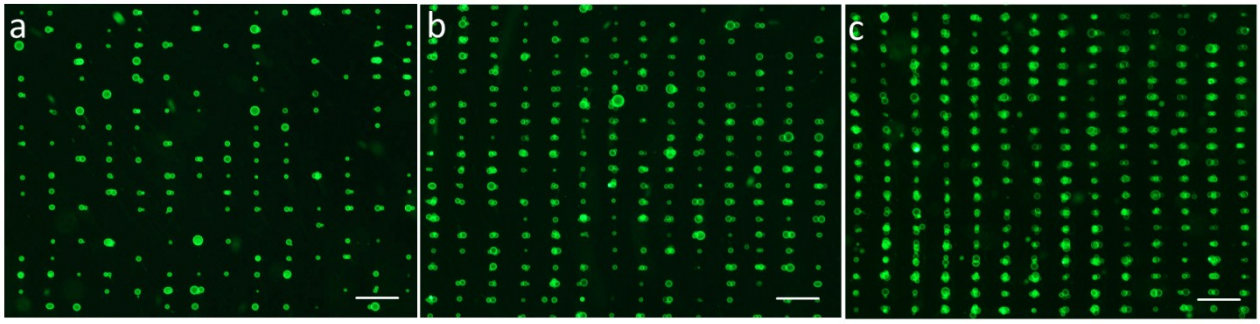


**Figure S9.** Representative fluorescence microscopy images of rectangular DOPC GUV micro-arrays prepared at $R_{G/N}$ values of 1.2 (**a**), 2.2 (**b**) and 3.4 (**c**). The GUVs were prepared using DOPC labeled with 5% NBD-PE. The acoustic trapping device was operated at 5.06/9.13 MHz (10 V) for all experiments. All scale bars are 200 μm.

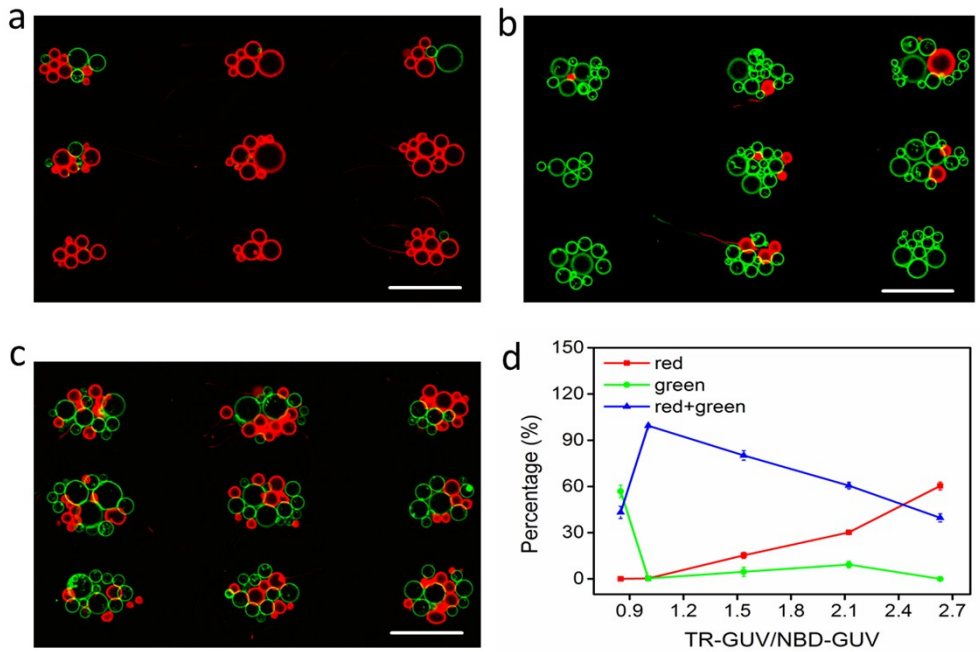


**Figure S10.** (**a-c**) Representative fluorescence microscopy images of acoustically trapped red (0.5% TR-DHPE) and green (5% NBD-PE) fluorescently labeled GUVs derived from binary populations containing number ratios (TR-GUV/NBD-GUV) of 2.6 (**a**), 0.85 (**b**) and 1.0 (**c**) for $R_{G/N}$ values of 3.6, 2.8 and 5.6, respectively. All scale bars are 100 μm. (**d**) Plots of the change in the percentage of nodes occupied by red, green or co-located red and green (blue line) fluorescent GUVs against TR/NBD. The acoustic trapping device was operated at 5.06/9.13 MHz (10 V) for all experiments. Three independent replicates were conducted in each number ratio (TR-GUV/NBD-GUV). Error bars represent the standard deviation.

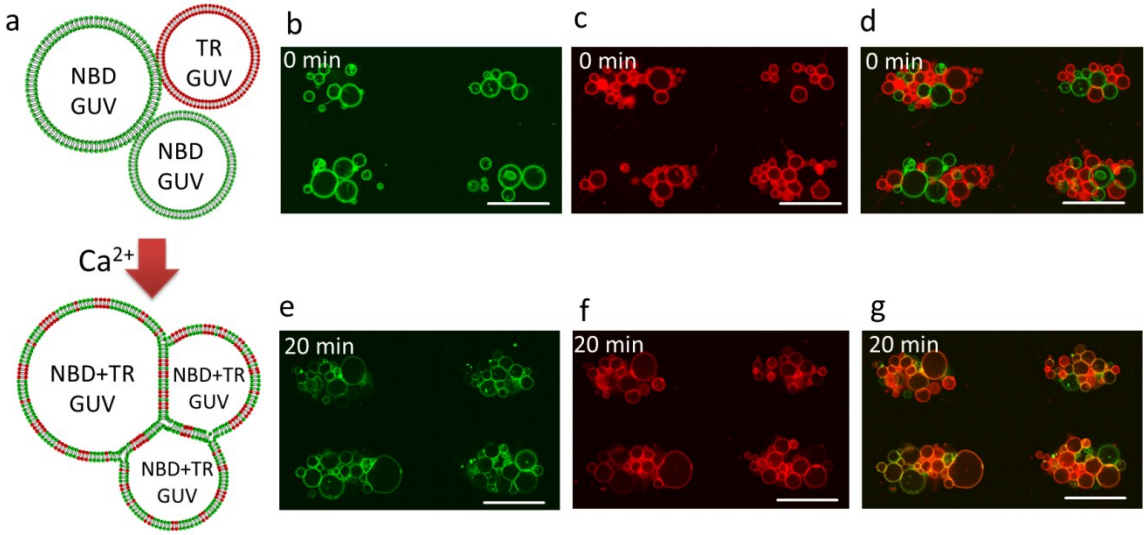


**Figure S11. Membrane hemifusion in the GUVs array.** (**a**) Schematic representation of the hemifusion process. (**b-d**) Representative fluorescence microscope images of heterogeneous GUVs array under 463 nm excitation for NBD labeled GUVs (**b**), 580 nm excitation for TR-DHPE labeled GUVs (**c**), and (**d**) for the superposition of (**b**) and (**c**), and corresponding fluorescence microscope images(**e-g**) of the same GUVs array as shown in (**b-d**) after addition of $CaCl_2$ (10 ul, 133 mM) for 20 min. All the GUVs in the 2D array had the same composition of the fluorescent lipid due to the lipid exchange suggesting the cluster GUVs at each node were successfully hemifused after the addition of $CaCl_2$. The GUVs were prepared from DOPC with 5% NBD-PE for the green fluorescence vesicles or with 0.5% TR-DHPE for the red fluorescence vesicles. The 2D heterogeneous GUVs array was prepared at 5.06/9.13 MHz (10 V). All scale bars are 50 μm.

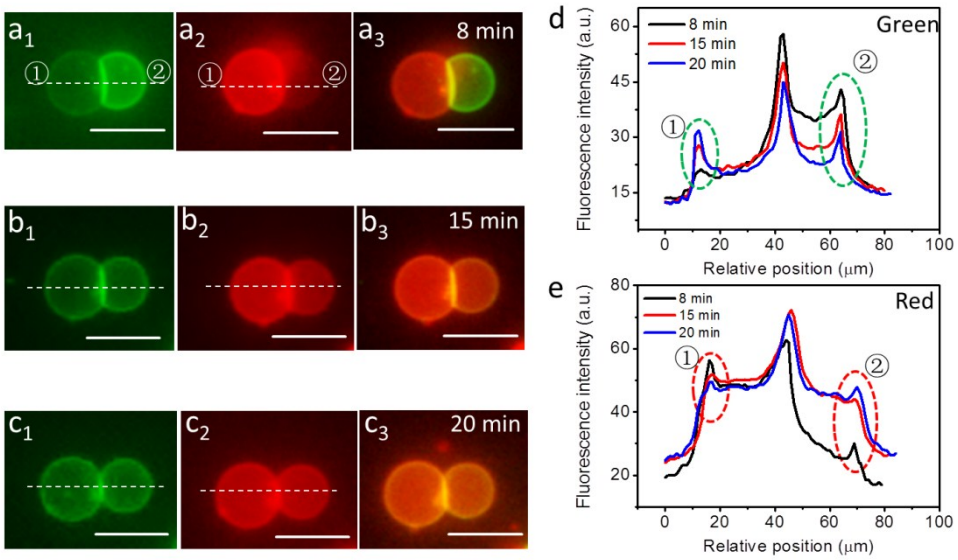


**Figure S12**. (**a-c**) Fluorescence microscopy images of a red-green fluorescence pair of trapped and hemifused GUVs recorded 8 (**a,** black), 15 (**b,** red) and 20 (**c,** blue) min after addition of $CaCl_2$; 463 nm excitation (**$a_1$, $b_1$, $c_1$**, green), 580 nm excitation (**$a_2$, $b_2$, $c_2$**, red) and superimposed images (**$a_3$, $b_3$, $c_3$**). Scale bars are 25 μm. (**d,e**) Line profiles showing time-dependent changes in green (**d**) or red (**e**) fluorescence intensity for the pair of trapped GUVs shown in **a-c**; labels **1** and **2** refer to the locations shown in **a-c.**

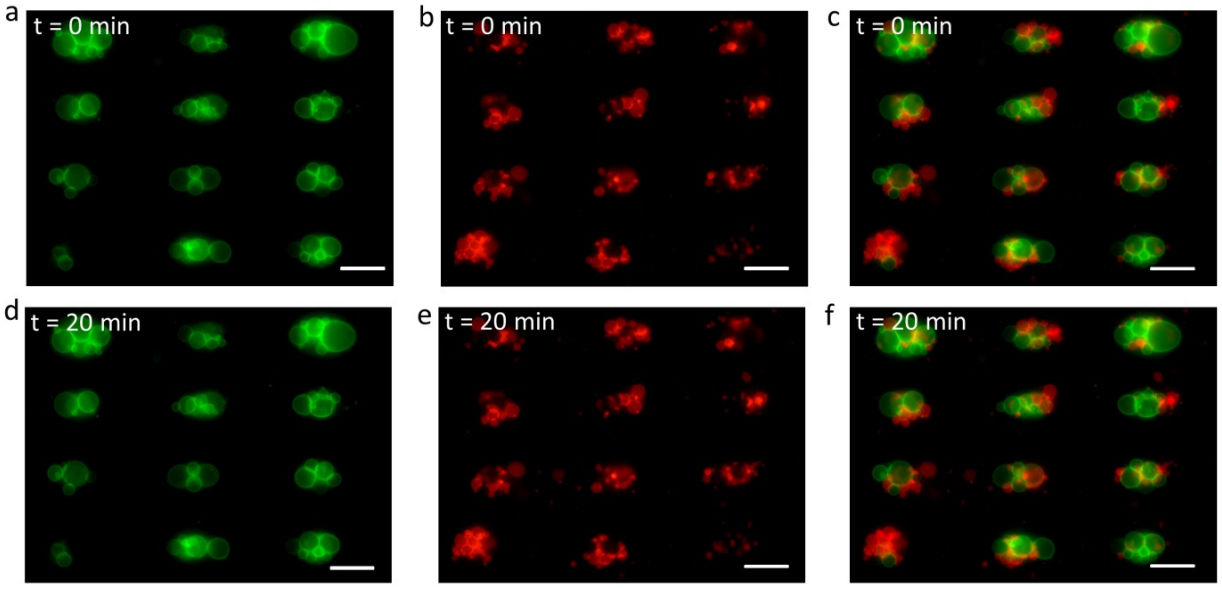


**Figure S13**. (**a-c**) Representative fluorescence microscopy images of a rectangular micro-array consisting of co-localized clusters of trapped green (5% NBD-PE) or red (0.5% TR-DHPE) fluorescent-labelled DOPC GUVs in the absence of $Ca^{2+}$. Images are recorded under 463 nm excitation (NBD-PE) (**a**) or 580 nm excitation (TR-DHPE) (**b**); superposition of **a** and **b** is shown in (**c**). (**d-f**) Corresponding fluorescence microscopy images of the same GUV micro-array as shown in **a-c**, but 20 min later showing no evidence for lipid exchange, consistent with the presence of non-fused vesicles. All scale bars are 50 μm. The acoustic trapping device was operated at 5.06/9.13 MHz (10 V).

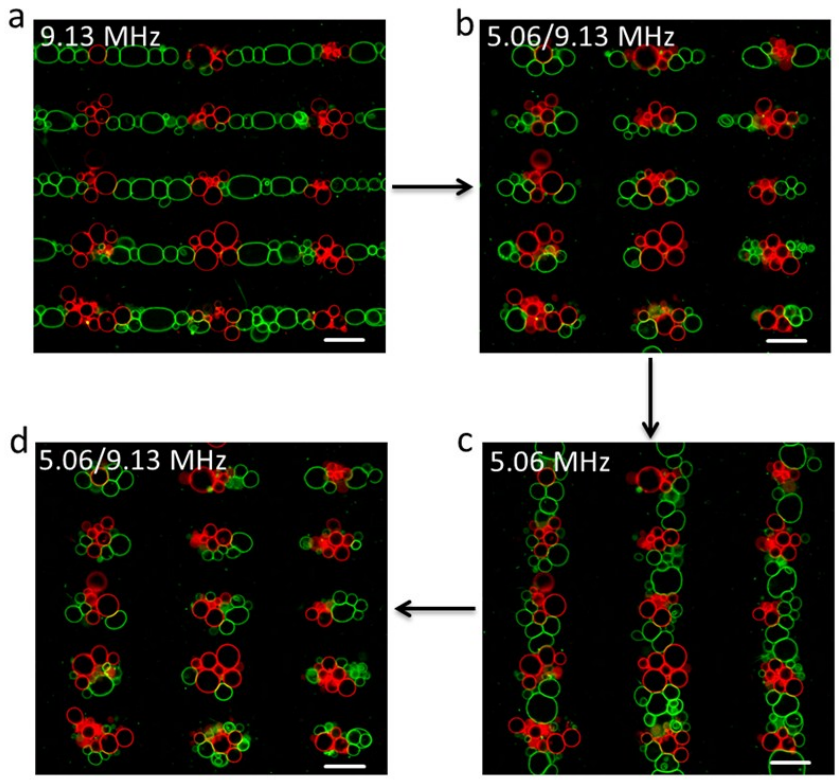


**Figure S14**. Representative fluorescence microscope images of dynamically modulated GUVs arrays containing hemifused GUVs (red fluorescence, labelled with 0.5% TR-DHPE) and non-fused GUVs (green fluorescence, labelled with 5% NBD-PE) under different acoustic fields; (**a**) 9.13 MHz, (**b**) 5.06/9.13MHz, (**c**) 5.06 MHz, (**d**) 5.06/9.13 MHz. Modulations in the acoustic field induce local migration of the non-fused GUVs (green) within a spatially fixed population of hemifused GUVs (red). Acoustic fields were switched on/off after 60 s. All scale bars are 50 μm.

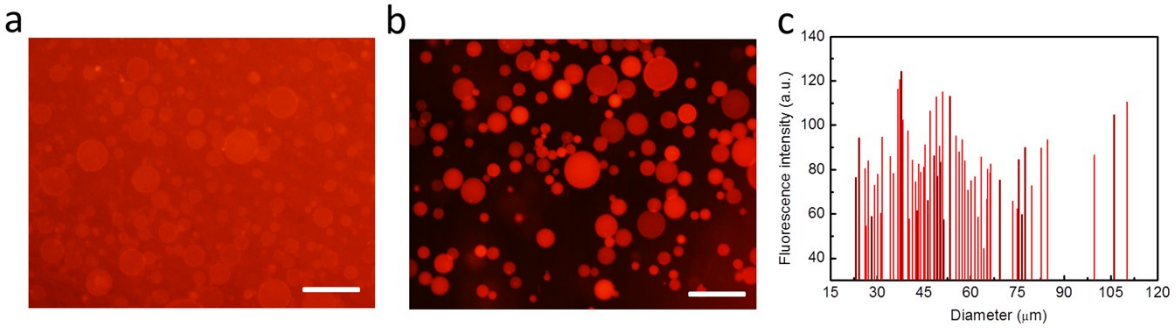


**Figure S15**. (**a**) Fluorescence microscopy image of sucrose (400 mM)-containing DOPC GUVs with encapsulated aqueous RITC-HRP (0.05 mg/mL) after electroformation showing red fluorescence inside and outside the vesicles. (**b**) Sample in **a** after washing three times with 400 mM glucose to remove RITC-HRP from the external continuous phase. Intact GUVs with HRP-entrapped aqueous interiors are observed. All scale bars, 100 μm. (**c**) Fluorescence intensity distribution against GUV diameter showing a relatively uniform distribution of HRP independent on the size of the GUVs. The mean florescence intensity is 80.14 ± 16.26.

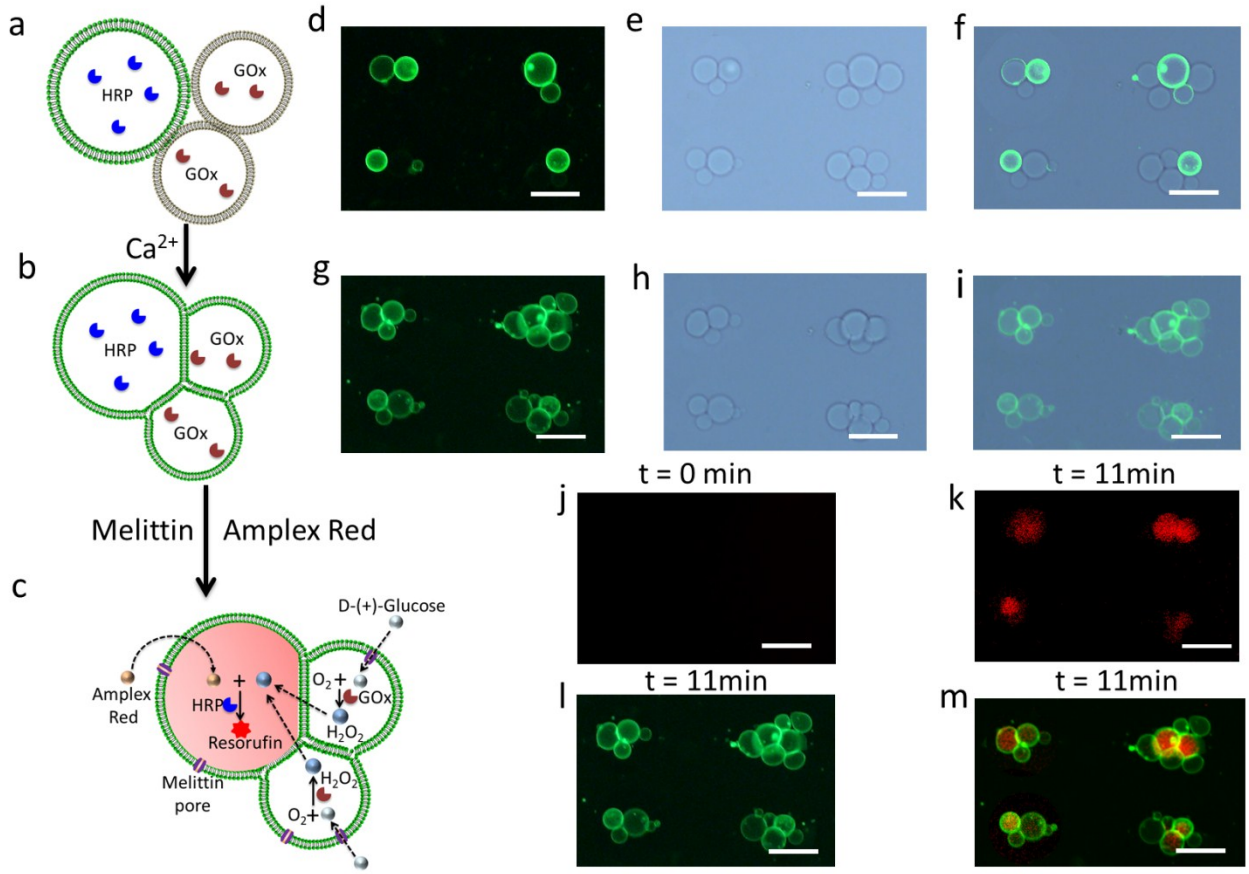


**Figure S16**. (**a-c**) Schematic representation of three acoustically co-trapped GUVs containing either GOx (two GUVs) or HRP (one GUV) and surrounded by an aqueous solution of glucose (1 mL, 400 mM) before (**a**) and after $Ca^{2+}$-induced (10 µL, 133 mM) hemifusion (**b**). Amplex red and melittin are added, and the enzyme cascade reaction is initiated by melittin incorporation into the lipid bilayer followed by addition and uptake of glucose (**c**). (**d-i**) Representative fluorescence (**d,g**) and bright field microscopy (**e,h**) images, and their superpositions (**f,i**) for a rectangular micro-array consisting of four spatially separated clusters of NBD-PE-labelled HRP-containing GUVs (green fluorescence, 463 nm) and unlabeled GOx-containing GUVs before (**d-f**) and after (**g-i**) hemifusion (GUV number ratio, 1:1). Hemifusion results in minimal displacement of the GUVs in each cluster and the onset of green fluorescence in the GOx-containing GUVs due to transfer of NBD-PE between the conjoined vesicles. (**j-k**) As for (**g**) but recorded at an excitation wavelength of 560 nm (red fluorescence) before (**j**) and 11 min after addition of Amplex red, glucose and melittin (**k**); corresponding green fluorescence image of (**k**) is shown in (**l**) and the superimposition of the red and green fluorescence images recorded after 11 min is displayed in (**m**). Production of resorufin as an output of the cascade reaction occurs specifically in the HRP-containing GUVs. All scale bars are 50 µm. The acoustic trapping device was operated at 5.06/9.13 MHz (10 V).

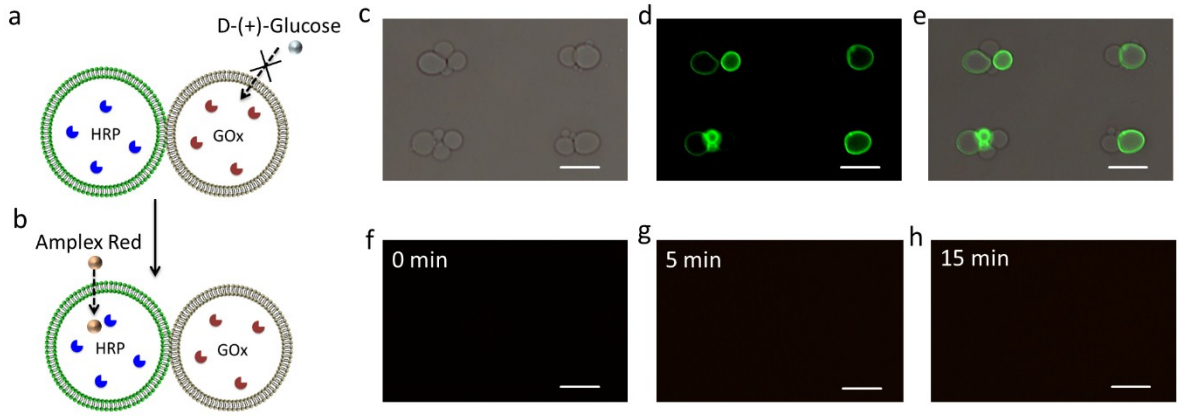


**Figure S17.** (**a,b**) Schematic representation of a control experiment showing Amplex red uptake and impermeability of glucose in acoustically trapped GUVs containing either HRP or GOx. The membrane pore-forming peptide melittin is absent. (**c-e**) Corresponding bright field image (**c**) and fluorescence microscopy image (**d**), and superposition of **c** and **d** (**e**) for a rectangular micro-array consisting of spatially separated clusters of co-trapped NBD-PE-labelled HRP-containing GUVs (0.1 U/mL; green fluorescence, 463 nm) and unlabeled GOx-containing GUVs (1 U/mL); GUV number ratio = 1:1. (**f-h**) Fluorescence microscopy images of the micro-array shown in **c-e** under 560 nm excitation 0 (**f**), 5 (**g**) and 15 min (**h**) after addition of Amplex red. All scale bars are 50 µm. Absence of red fluorescence indicates that the cascade is not activated due to the membrane impermeability of glucose in the absence of the porogen. The acoustic trap was operated at 5.06/9.13MHz (10 V).

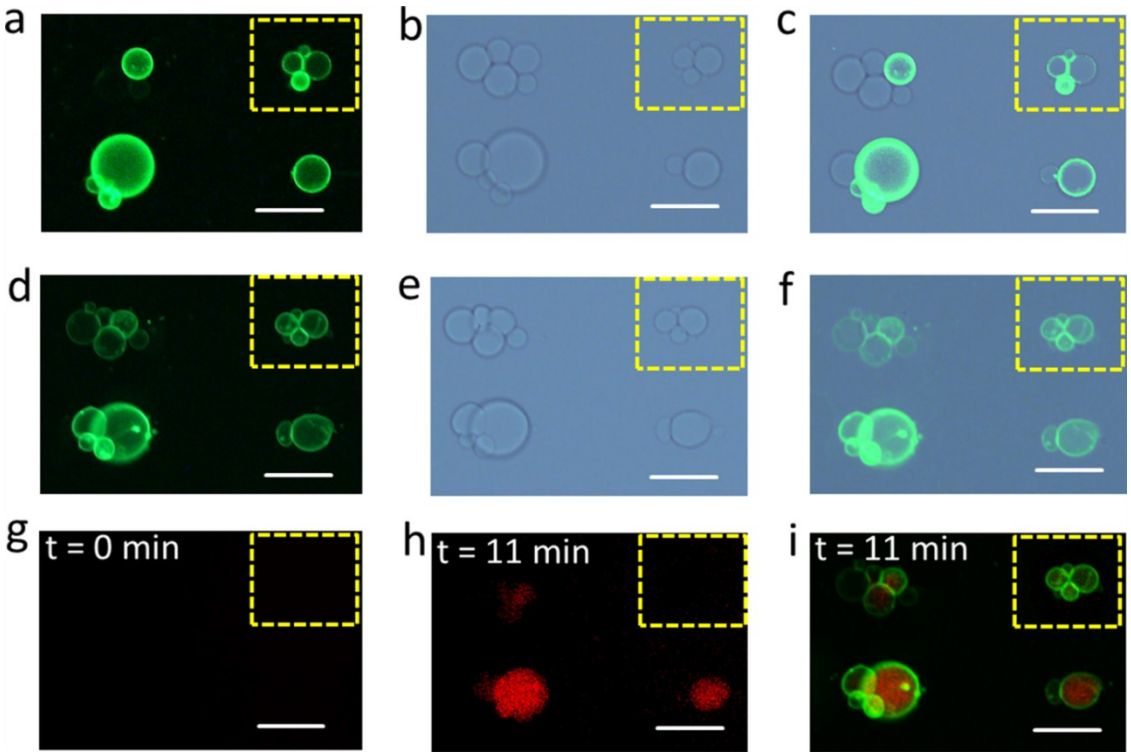


**Figure S18.** (**a-f**) Representative fluorescence (**a,d**) and bright field microscopy (**b,e**) images, and their superpositions (**c,f**) for a rectangular micro-array consisting of four spatially separated clusters of multiple NBD-PE-labelled HRP (0.1 U/mL)-containing GUVs (green fluorescence, 463 nm) and unlabeled GOx (1 U/mL)-containing GUVs before (**a-c**) and after (**d-f**) hemifusion ($CaCl_2$, 10 µL, 133 mM; GUV number ratio, 1:1). The dashed yellow box delineates a cluster containing only HRP-containing GUVs as shown by the equivalence of the fluorescence and optical images in this region of **a** and **b**. (**g-i**) As for (**d**) but recorded at an excitation wavelength of 560 nm (red fluorescence) before (**g**) and 11 min after addition of Amplex red, glucose and melittin (**h**); corresponding superimposition of the red and green fluorescence images recorded after 11 min is displayed in (**i**). Production of resorufin occurs specifically in the HRP-containing GUVs that are connected to GOx-loaded GUVs; thus, the cluster of GUVs delineated by the yellow dashed box shows no fluorescence output. All scale bars are 50 µm. The acoustic trapping device was operated at 5.06/9.13 MHz (10 V).

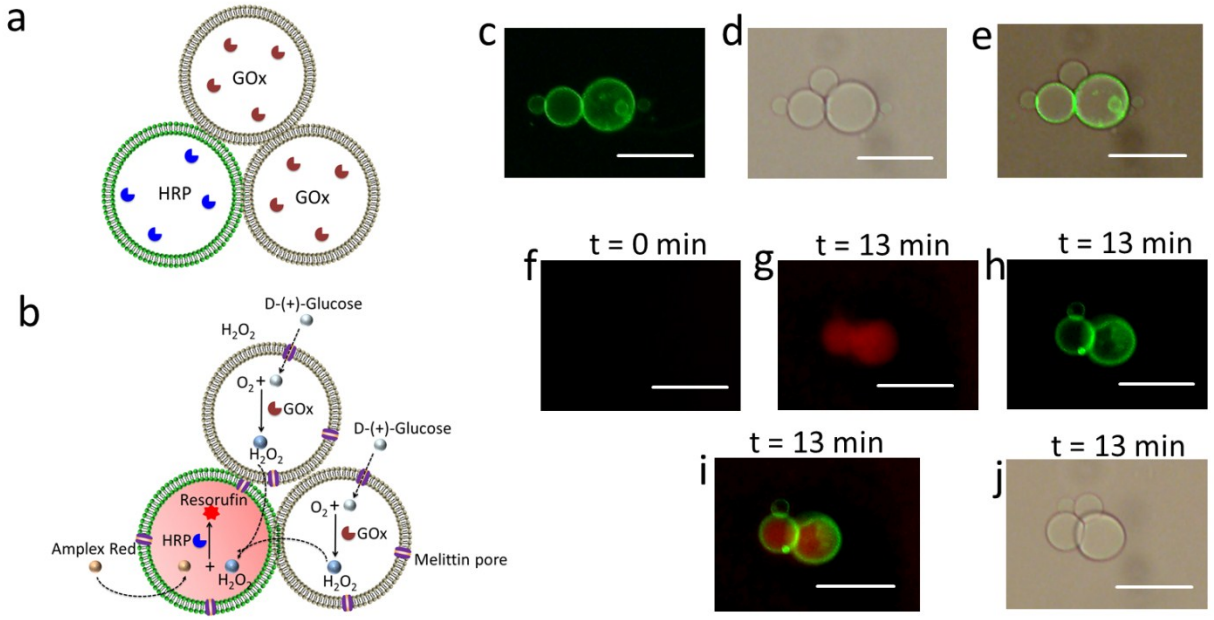


**Figure S19.** (**a,b**) Schematic representation of a GOx/HRP enzyme cascade in non-hemifused acoustically co-trapped GUV micro-array in the presence of melittin (5 µL, 800 µg/mL), glucose (1 mL, 400 mM) and Amplex red (10 µL, 50 µM). (**c-e**) Representative fluorescence (**c**) and bright field microscopy (**d**) images, and their superposition (**e**) showing two NBD-PE-labelled HRP-containing GUVs (green fluorescence, 463 nm) and a single unlabelled GOx-containing GUV s trapped at the same acoustic pressure node. (**f-j**) As for (**c-e**) but recorded at an excitation wavelength of 560 nm (red fluorescence) before (**f**) and 13 min after addition of Amplex red, glucose and melittin (**g**); corresponding green fluorescence (463 nm) image of (**g**) is shown in (**h**) and the superimposition of the red and green fluorescence images recorded after 13 min is displayed in (**i**) along with the optical image at 13 min (**j**). Production of resorufin as an output of the cascade reaction occurs specifically in the HRP-containing GUVs. Production of resorufin as an output of the cascade reaction occurs specifically in the two HRP-containing GUVs. All scale bars are 50 µm. The acoustic trapping device was operated at 5.06/9.13 MHz (10 V).

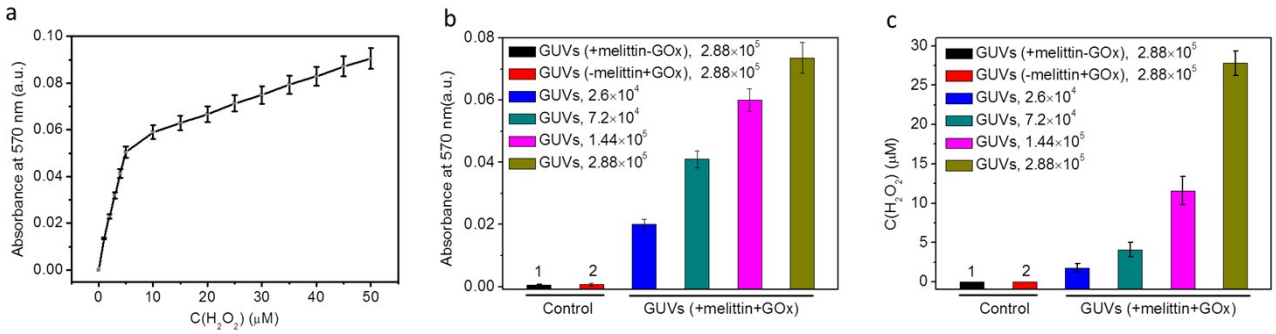


**Figure S20**. Determination of the $H_2O_2$ flux associated with melittin-functionalized GOx-containing GUV activity. (**a**) Calibration curve of the absorbance at 570 nm (resorufin production) at different concentrations of $H_2O_2$ using an Amplex red assay ([Amplex red] = 50 µM; [HRP] = 2.5 U/mL). Three independent replicates were conducted in each $H_2O_2$ concentration. Error bars represent the standard deviation. (**b**) Bar plots of the absorbance at 570 nm (resorufin production) against the number of melittin-functionalized GOx-containing GUVs ($2.6 \times 10^4$ to $2.88 \times 10^5$) added to a mixture of Amplex red, glucose and HRP (100 µL, 50 µM, 30 mM and 2.5 U/mL, respectively). Data were recorded after 60 min. Production of resorufin increased as the number of added GUVs increased. Control experiments in the absence of melittin or GOx showed minimal cascade reactivity due to the impermeability of glucose across the GUV membrane and concomitant absence of a $H_2O_2$ efflux. (**c**) Bar plots of the concentration of $H_2O_2$ as shown in (**b**) derived from the calibration shown in (**a**). Three independent replicates were conducted in each experimental group and control group. Error bars represent the standard deviation.

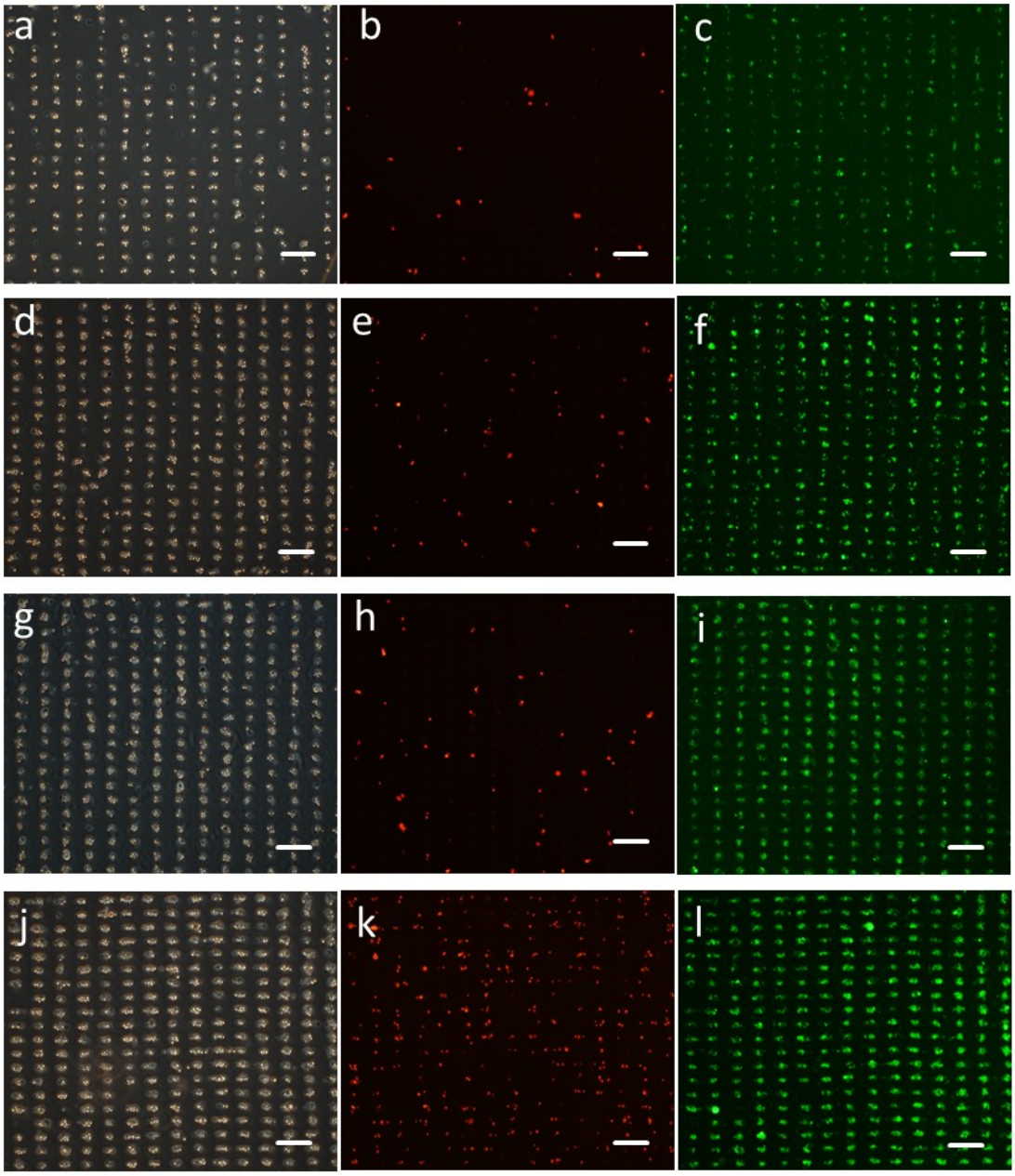


**Figure S21.** (**a-c**) Representative bright field image (**a**) and fluorescence microscopy images recorded at 535 nm excitation (red fluorescence, PI-DNA stained; dead HepG2 cells) (**b**) and 463 nm (green fluorescence, 5% NBD-PE labelled GUVs (**c**) of co-localized melittin-functionalized GOx containing GUVs and HepG2 cells recorded 4 h after addition of glucose (100 μL, 300 mM; 1 mL medium) at a GUV/HepG2 number ratio of 0.5. As shown in (**a-c**), but at GUV/HepG2 number ratios of 1.4 (**d-f**), 2.9 (**g-i**) and 5.7 (**j-l**). The number of HepG2 cells was approximately 56,000 in all experiments. The acoustic trapping device was operated at 5.06/9.13 MHz (10 V). Cells were stained for 20 min with PI PBS solution (20 μL, 20 μg/mL) after 4 h incubation in glucose. All scale bars are 200 μm.

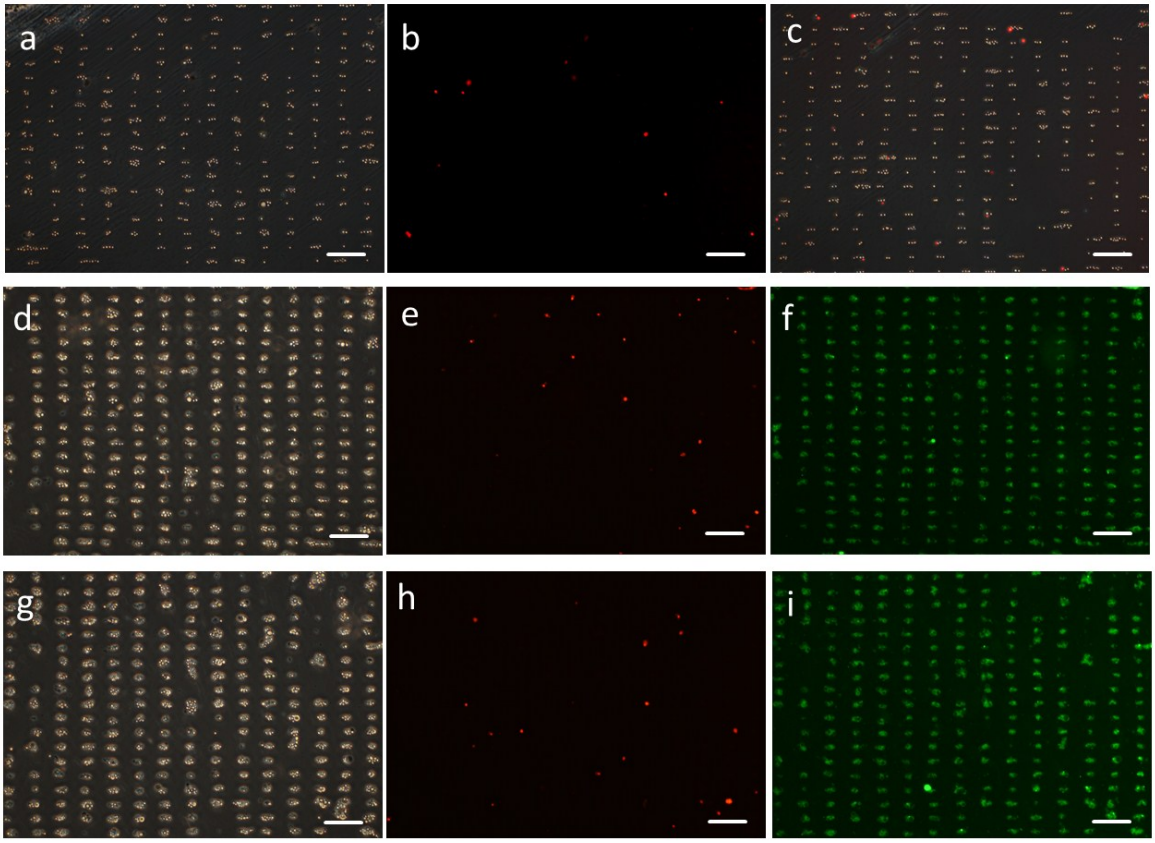


**Figure S22.** Control experiments**.** (**a-c**) HepG2 cancer cells and glucose (no GUVs, no GOx, no melittin). Representative bright field image (**a**), corresponding fluorescence microscopy image recorded under 535 nm excitation (red fluorescence, PI-DNA stained; dead HepG2 cells) (**b**), and superimposed images (**c**) of an acoustically trapped homogeneous micro-array of HepG2 cancer cells incubated for 4 h in cell medium with 30 mM glucose and then stained with PI. (**d-f**) Melittin-functionalized GUVs (no GOx), HepG2 cells and glucose. Representative bright field image (**d**), and corresponding fluorescence microscopy images recorded under 535 nm excitation (red fluorescence, PI-DNA stained; dead HepG2 cells) (**e**), and under 463 nm excitation (green fluorescence, 5% NBD-PE labelled GUVs) (**f**) of acoustically co-trapped melittin-functionalized GUVs (no GOx) and HepG2 cells incubated for 4 h in cell medium with 30 mM glucose and then stained with PI at a GUV/HepG2 number ratio of 5.7. (**g-i**) GOx-containing GUVs (no melittin), HepG2 cells and glucose. Image modes as shown in (**d-f**). In all cases, very few dead cells were observed. The number of HepG2 cells was approximately 56,000 in all experiments. The acoustic trapping device was operated at 5.06/9.13 MHz (10 V). Cells were stained for 20 min with PI PBS solution (20 µL, 20 µg/mL) after 4 h incubation in glucose. All scale bars are 200 µm.

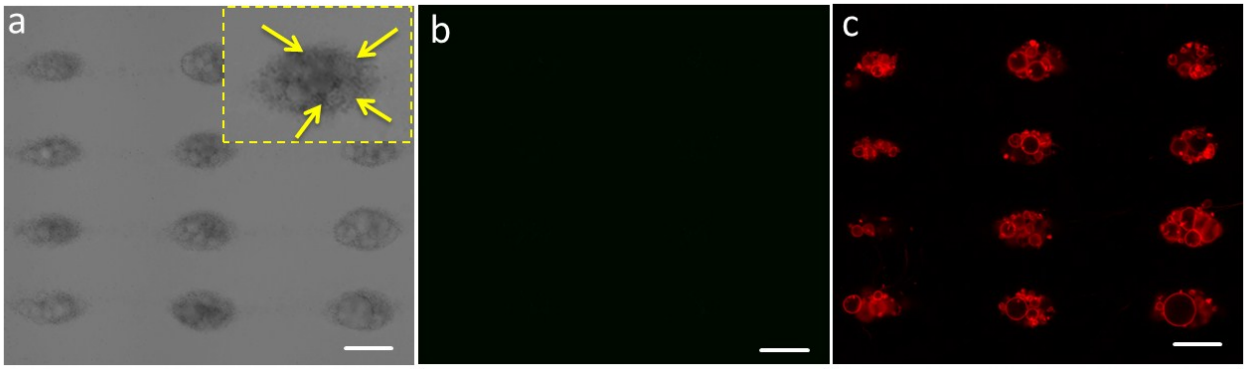


**Figure S23**. Representative bright field image (**a**) and fluorescence microscopy images recorded at 463 nm excitation (green fluorescence) (**b**) and 535 nm (red fluorescence, 0.5% TR-DHPE labelled GUVs) (**c**) of co-localized non-IPTG containing GUVs and *E.coli* recorded 6 h after the addition of melittin. All scale bars are 50 µm. The darker dots observed at the nodes (yellow arrows in the inset in (**a**)) are *E.coli* cells. Image **b** indicates no GFP expression in *E.coli* in the absence of IPTG inside GUVs.

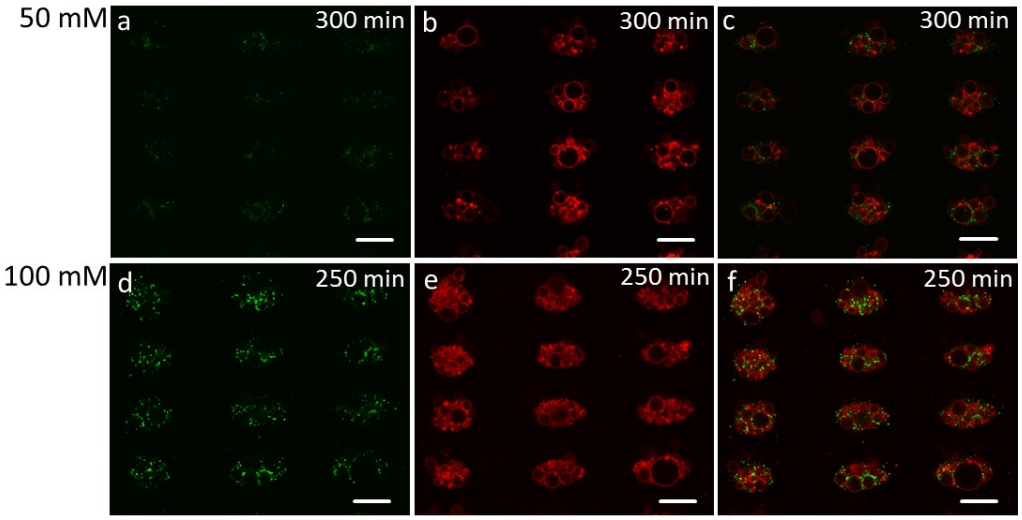


**Figure S24**. (**a-c**) Representative fluorescence microscopy images recorded at 463 nm excitation (green fluorescence) (**a**), 535 nm (red fluorescence, 0.5% TR-DHPE labelled GUVs) (**b**), and superimposition of **a** and **b** (**c**) of co-localized GUVs (containing 50 mM ITPG) and *E.coli* recorded 300 min after the addition of melittin. (**d-f**) Representative fluorescence microscopy images recorded at 463 nm excitation (green fluorescence) (**d**), 535 nm (red fluorescence, 0.5% TR-DHPE labelled GUVs) (**e**), and superimposition of **d** and **e** (**f**) of co-localized GUVs (containing 100 mM ITPG) and *E.coli* recorded 250 min after the addition of melittin. All scale bars are 50 µm.

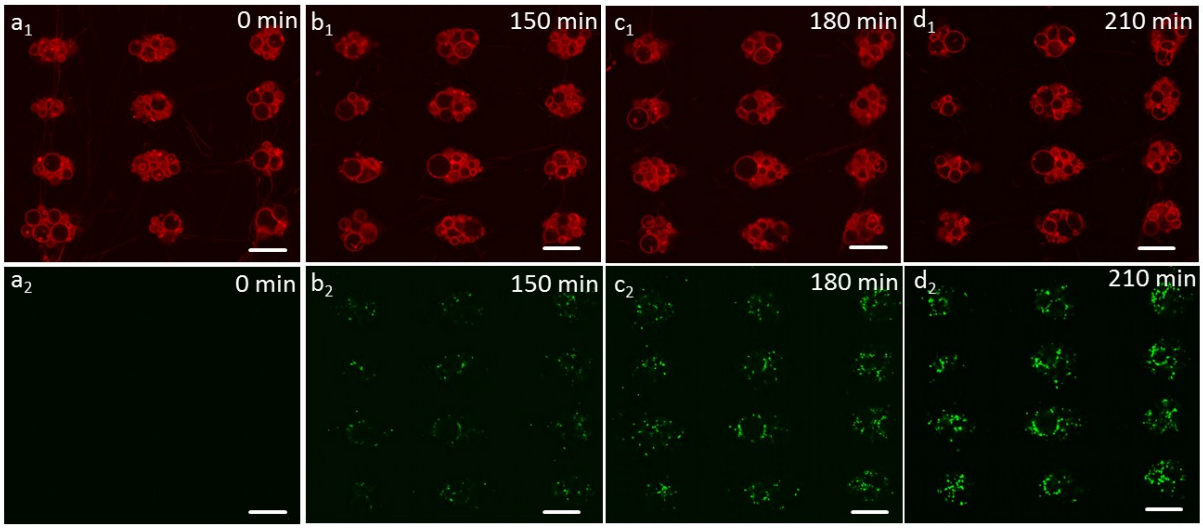


**Figure S25**. Representative fluorescence microscopy images recorded at 535 nm excitation (red fluorescence, 0.5% TR-DHPE labelled GUVs) (**$a_1$-$d_1$**), 463 nm (green fluorescence) **($a_2$-$d_2$)** of co-localized GUVs (containing 150 mM ITPG), and *E.coli* recorded 0 min (**$a_1$, $a_2$**), 150 min (**$b_1$, $b_2$**), 180 min (**$c_1$, $c_2$**), 210 min (**$d_1$,$d_2$**) after the addition of melittin. All scale bars are 50 μm.

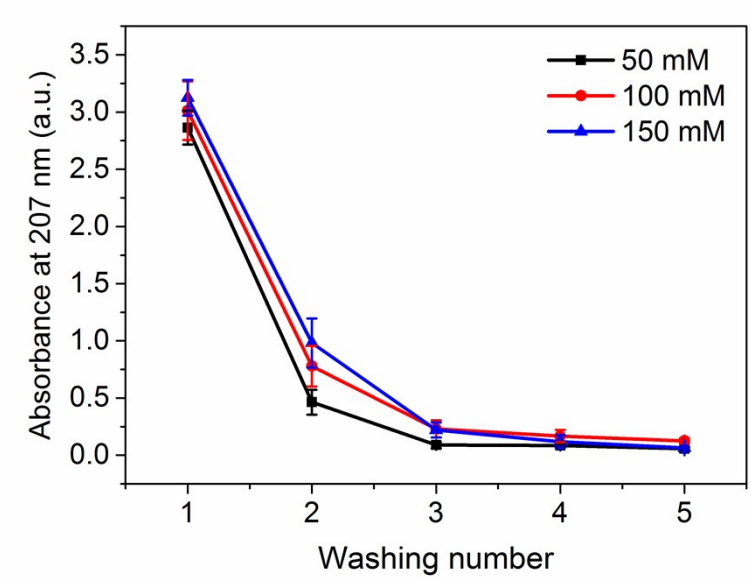


**Figure S26**. Plots of UV/Vis absorption at 207 nm in the washings (50 (black), 100 (red), 150 (blue) mM) showing there was no residual IPTG in the continuous phase. Three independent replicates were conducted in each IPTG concentration. Error bars represent the standard deviation.

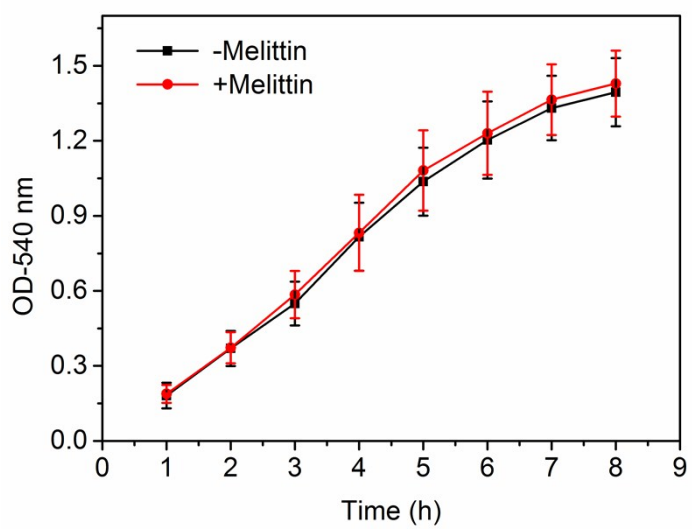


**Figure S27.** Growth curves of *E. coli* with (black) and without (red) melittin for 8h. A pre-cultured *E. coli* solution (450 μL) was dispersed into 2.55 mL liquid medium. Experimental group (three replicates) containing melittin (final concentration, 4 μg/mL) and the control group (three replicates) without melittin were incubated at 37 ℃. Optical density at 540 nm was measured every 1 h. Error bars represent the standard deviation.

## References

[1] C. R. P. Courtney *et al.*, Manipulation of particles in two dimensions using phase controllable ultrasonic standing waves. *Proc. R. Soc. A*, **2011**, *468*, 337-360.